THE BELL SYSTEM TECHNICAL JOURNAL
Vol. 50, No. 6, July-August, 1971
Printed in U.S.A.

A Nonlinear Diffusion Analysis of Charge-Coupled-Device Transfer

By R. J. STRAIN and N. L. SCHRYER

(Manuscript received January 25, 1971)

In those charge-coupled devices (CCD's) which have regions under each electrode which are substantially free of externally applied tangential electric fields, charge motion takes place by space charge assisted diffusion, and this relatively slow process represents a limitation to the operating frequency of CCD's with large plates. In this paper, subject to certain approximations, the equations of motion for CCD charge transfer have been derived, yielding a nonlinear diffusion equation. The solution of this equation by a stable finite difference scheme is described, and the solutions are applied to predicting the operating characteristics of CCD's. The results in synopsis are:

(*i*) *The n-channel devices will have lower losses at a given frequency than the p-channel devices, and a higher upper frequency limit.*
(*ii*) *Higher amplitude signals (more charge) yield lower losses.*
(*iii*) *Losses can be reduced an order of magnitude by using* ZERO*'s which carry a substantial amount of charge. For example, with 2-MHz clocking of a 25-μm plate (pad), p-channel 2-phase device, a 2-volt* ONE *is diminished by 4 percent per transfer with empty* ZERO*'s, but with 1-volt* ZERO*'s, the diminution is 0.26 percent per transfer.*
(*iv*) *Reasonably efficient CCD operation should be possible up to the 50-MHz range using contemporary design tolerances.*
(*v*) *Diffusion is important for reaching high transfer efficiencies.*

The frequency limitations described in this paper can be overcome by using a structure in which the distance between the electrodes and transferring charge is comparable to the electrode width and spacing.

I. INTRODUCTION

The charge-coupled device, as conceived by Boyle and Smith[1] and realized by Amelio, Tompsett, and Smith,[2,3] consists of a series of

metal oxide semiconductor (MOS) capacitors that are driven by clock pulses into deep depletion. In this condition, the MOS structures are capable of holding minority carriers in the potential wells beneath the plates (pads). In order to establish a transfer of charge from one plate to another, it is necessary to make the potential well beneath the second plate deeper than that beneath the first. This is illustrated in Fig. 1. In the absence of charge, the potential configuration beneath any one plate would be essentially flat, and finite electric fields would exist only in that span between two CCD electrodes. When charge is present, its transfer is driven predominately by the electrostatic forces associated with the presence of the charge in the CCD and by the thermal forces responsible for diffusion. It is the purpose of this paper to describe the transport of charge under the influence of these forces and, using this description, to make predictions concerning the operation of CCD's. In order to do this, it will be necessary first to derive the equation governing the transport of charge and solve it. Then the solutions will be applied to some particular CCD situations.

II. DERIVATION OF TRANSPORT EQUATION

The derivation of the transport equation will utilize a number of approximations. The first of these is a linear approximation of

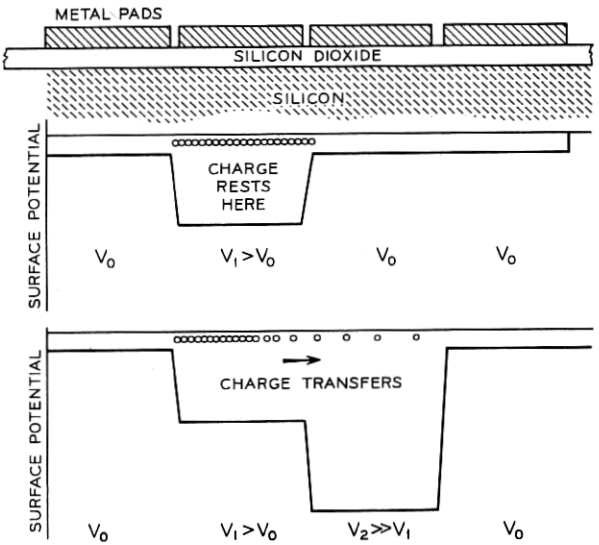

Fig. 1—A diagram of a CCD cross section and surface potential diagrams illustrating charge storage and charge transfer in CCD's.

the surface potential versus applied voltage relationship. The one-dimensional relationship between surface potential φ and applied voltage V_A is described by this equation:

$$\begin{aligned} \varphi &= V' + V_0 - \sqrt{V_0^2 + 2V_0V'} \\ V' &= V_A - V_{FB} = \frac{q}{C_{ox}} \\ V_0 &= \delta^2 e N_D \frac{\epsilon_s}{\epsilon_{ox}} \\ C_{ox} &= \frac{\epsilon_{ox}}{\delta}. \end{aligned} \tag{1}$$

In this equation V_{FB} is the MOS flatband voltage, and q is the surface density of mobile charge stored at the interface between the silicon and silicon dioxide. The constant V_0 depends upon the oxide thickness δ, the doping density N_D, the dielectric constant ε_{ox} of the oxide, and the dielectric constant ε_s of the silicon. In the subseqeunt calculations, however, an approximation to this relationship will be used which is linear in V_A and q. This approximation is

$$\varphi = \varphi_0 + \gamma\left(V_A - V_{FB} + \frac{q}{C_{ox}}\right). \tag{2}$$

In this case γ is a number, typically between 0.7 and 1, which matches equation (2) to equation (1) over the range of anticipated operation. Such a match is shown in the example of Fig. 2, which shows the surface potential versus applied voltage reduced by the flatband voltage and q/C_{ox}, both in the precise form and in the linear approximation. It may be seen in this case that the linear approximation is rather good over the range from approximately 4 to 15 volts. If the electric field parallel to the Si-SiO_2 interface is calculated from the approximate equation, it is found to depend upon the derivative of q. There is, however, another term to the tangential electric field; this term arises from the electrostatic repulsion of the carriers. In a two-dimensional approximation, the tangential electric field at x will have a component due to the summation of the fields of line charges located at other points x' along the surface. Because there is a metallic electrode on the surface of the SiO_2, each elemental line charge has an image, and the result is a shielding of the tangential field. Taking account of the two different dielectrics and the image charge, the repulsion field E_R can be written as this integral:

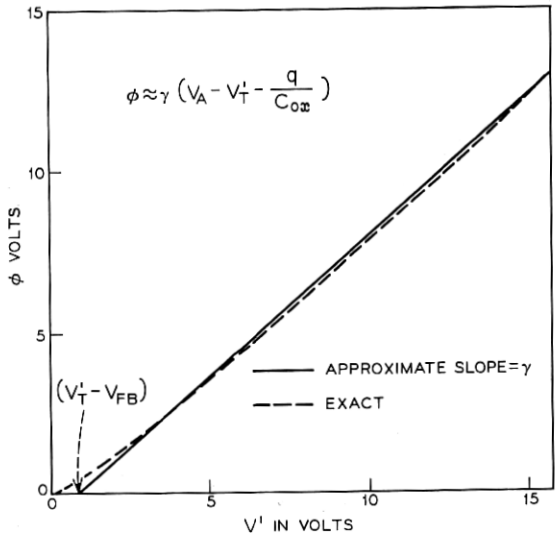

Fig. 2—The exact variation of deep depletion surface potential in an MOS with 1000Å of SiO_2 over a substrate with 5×10^{14} ionized impurities per cm^3, and the linear approximation $\Phi \propto \gamma V'$.

$$E_R(x) = \pi(\epsilon_{ox} + \epsilon_s) \int q(x') \left\{ \frac{1}{x - x'} - \frac{x - x'}{(x - x')^2 + 4\delta^2} \right\} dx'. \tag{3}$$

Since the principal contribution to this integral comes from the small region within a few δ of x, it is appropriate to expand $q(x')$ as a Taylor series about x. If this is done, and the limits of integration are extended over all x', all even terms in the expansion vanish by symmetry, and to the extent that $\partial^3 q/\partial x^3$ and higher derivatives are negligible, the repulsion field becomes a local function of $\partial q/\partial x$.

$$E_R(x) = -\frac{2\delta}{\epsilon_{ox} + \epsilon_s} \frac{\partial \delta}{\partial x}. \tag{4}$$

If one takes the gradient of equation (2) and adds the repulsion field in equation (4), the total electric field acting on the charge under the CCD plate is given by

$$\begin{aligned} E_x &= -S \frac{\partial q}{\partial x} \\ S &= \left(\frac{\gamma \delta}{\epsilon_{ox}} + \frac{2\delta}{\epsilon_s + \epsilon_{ox}} \right). \end{aligned} \tag{5}$$

Typical values of both γ and the net elastance S are presented in Figs. 3 and 4 as functions of the oxide thickness δ. Ordinarily S is approximately equivalent to the reciprocal of the oxide capacitance; consequently, Fig. 4 has been plotted in such a way that the value of S is compared with the oxide capacitance.

The transport equation for CCD's will be based on the divergence equation for current

$$\frac{\partial q}{\partial t} = -\nabla \cdot J, \tag{6}$$

using the relationship

$$J = q\mu E - D\frac{\partial q}{\partial x} \tag{7}$$

for the value of the current density J. In this equation D is the diffusion coefficient appropriate to the surface, and μ is the surface mobility. Combining equations (5), (6), and (7) gives the basic equa-

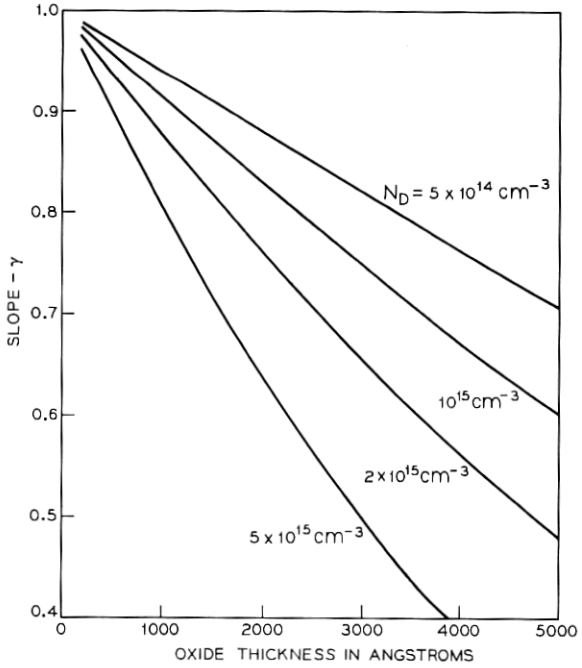

Fig. 3—The proportionality constant γ as a function of oxide thickness, using doping density as a parameter.

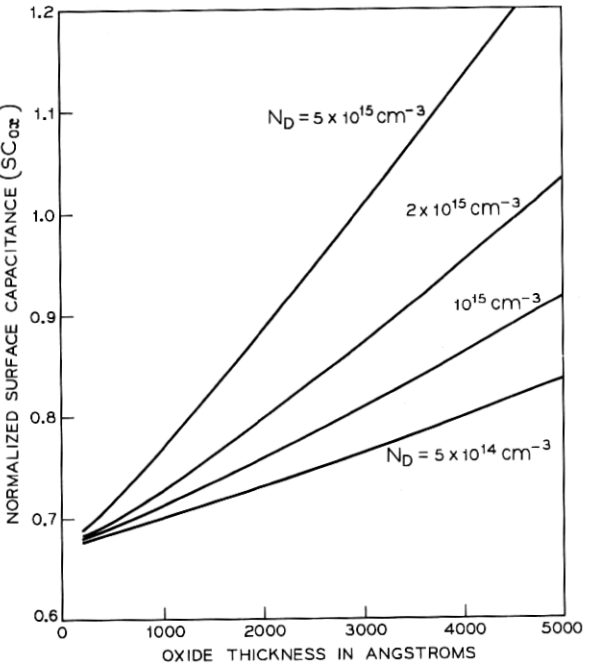

Fig. 4—The effective surface capacitance, $1/S$ (the reciprocal of elastance S) normalized by C_{ox} and presented as a function of oxide thickness.

tion for charge transport in a CCD:

$$\frac{\partial q}{\partial t} = \mu S\left(\frac{\partial q}{\partial x}\right)^2 + q\mu S\,\frac{\partial^2 q}{\partial x^2} + D\,\frac{\partial^2 q}{\partial x^2}. \tag{8}$$

This may be simplified somewhat by noting the Einstein relationship between diffusion and mobility.

$$D = \frac{\kappa T}{e}\,\mu. \tag{9}$$

Here κT and e all assume their traditional values as Boltzmann's constant, absolute temperature, and electronic charge. Using this substitution, one reaches this equation:

$$\frac{\partial q}{\partial t} = \mu S\left(\frac{\partial q}{\partial x}\right)^2 + \mu S q\,\frac{\partial^2 q}{\partial x^2} + \frac{\kappa T}{e}\,\mu\,\frac{\partial^2 q}{\partial x^2}. \tag{10}$$

The last term on the right of equation (10) is simply the diffusion

term. The resemblance between this diffusion term and the other term involving the second partial of charge is quite apparent, because the product Sq, like $\kappa T/e$, is a voltage.

Without boundary conditions, the problem is only half specified. The physical situation on which the boundary conditions are based is shown in Fig. 5. In Fig. 5a, a CCD plate is shown storing charge. The potential beneath the plate and the charge density are both uniform. In Fig. 5b, another potential well has been impressed immediately adjacent to the first potential well. The second well is considerably deeper than the first; as a consequence, charge will start to flow from the first potential well into the second under the control of equation (8). No charge, however, flows in the opposite direction. Between the two potential wells there is an abrupt step in potential. This means that there is an extremely high electric field, and charge in that vicinity will move with a very high velocity. Using the preceding facts, it is possible to approximate the physical boundary conditions in the

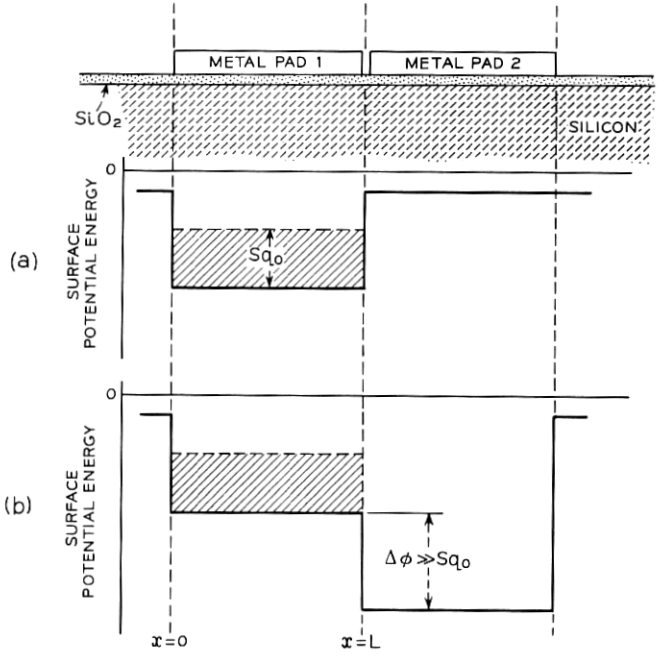

Fig. 5—An illustration of the length definition and the surface potential configuration in equilibrium, and at $t = 0$, when the transfer is initiated.

following way.

$$\frac{\partial q}{\partial x} \to 0 \quad \text{as} \quad x \to 0$$
$$q = 0 \quad \text{at} \quad x = L. \tag{11}$$

Both of these boundary conditions apply for all time. The first expresses the fact that current is unable to flow to the left in the device, and the second presumes either an ideal sink for charge at $x = L$, or alternatively that charge moves away from that point at an infinite velocity. The initial condition is a value of q at time $t = 0$ for all points except $x = L$; it will be assumed that the charge is evenly distributed with the magnitude q_0.

Before proceeding with the solution to this equation, it will be convenient to scale the variables. The scaling can be effected by applying the following definitions:

$$\tau = \frac{t}{\frac{L^2}{\mu \tau_0}} = \frac{t}{\tau_0} \tag{12a}$$

$$u_0 = 1 \text{ volt}$$

$$y = \frac{x}{L} \tag{12b}$$

$$u = \frac{Sq}{u_0}. \tag{12c}$$

Time is now represented by the variable τ, which scales time against τ_0, and y is the dimensionless variable representing length. In the definitions of τ and τ_0, the voltage unit u_0 is introduced. If this equation had a natural voltage unit, u_0 would be defined as that unit. However, there is no natural voltage scale to equation (10), even though the thermal voltage $\kappa T/e$ appears in one term; consequently, it has proven convenient to define u_0 to be unity. The quantity u representing charge comes about because the product of the elastances and charge q is equivalent to a voltage. In the solutions which follow τ will typically range from 10^{-2} to 10^2, y will range from 0 to 1, and u will range from 10^{-3} to 10.

III. SOLUTION OF THE EQUATION

The scaled equation has the form

$$u_\tau = u_y^2 + (u + a)u_{yy} \tag{13}$$

where $a = \kappa T/eu_0$ is a constant. The problem may be simplified by letting $w = u + a$ to obtain

$$w_\tau = w_y^2 + w_{yy}w \tag{14}$$
$$0 \leqq y \leqq 1$$
$$0 \leqq \tau \leqq \infty$$

subject to

$$w_y(0, \tau) = 0$$
$$w(1, \tau) = a$$
$$w(y, 0) = \begin{cases} u_i + a, & 0 \leqq y < 1 \\ a, & y = 1 \end{cases} \tag{15}$$
$$u_i = \frac{Sq_0}{u_0}$$

where u_i is determined by the initial uniform charge density q_0.

The nonlinear parabolic initial boundary value problem given by equation (14) and equation (15) may be solved using a finite difference scheme. The scheme comes from a more general technique for solving systems of coupled nonlinear parabolic equations which results in *linear* difference equations. This more general scheme will be published at a later date.

Let h be the space mesh size and $\Delta\tau$ be the time step. Let $w_j^k = w(jh, k\Delta\tau)$. The indices j and k describe position and time respectively. The difference equation is then:

$$\frac{w_j^{k+1} - w_j^k}{\Delta\tau} = \frac{1}{2}\left[\frac{w_{j+1}^{k+1} - w_{j-1}^{k+1}}{2h}\,\frac{w_{j+1}^k - w_{j-1}^k}{2h} + w_j^{k+1}\,\frac{w_{j+1}^k + w_{j-1}^k - 2w_j^k}{h^2}\right.$$
$$\left. + \frac{w_{j+1}^k - w_{j-1}^k}{2h}\,\frac{w_{j+1}^{k+1} - w_{j-1}^{k+1}}{2h} + w_j^k\,\frac{w_{j+1}^{k+1} + w_{j-1}^{k+1} - 2w_j^{k+1}}{h^2}\right], \tag{16}$$

for $j = 1, \cdots, J-1$, where $h = 1/J$. The boundary conditions reduce to $w_0^{k+1} = w_1^{k+1}$ and $w_J^{k+1} = a$.

This is a direct generalization of the Crank-Nicholson scheme for solving the heat equation, $w_t = w_{xx}$. For a description of that scheme and its properties, see Ref. 4, pp. 185–193.

The most important properties of (16) come from the time and

space averaging which is the hallmark of the Crank-Nicholson scheme. The left-hand side of (16) is close to the value of $w_t(jh, (k + 1/2)\Delta t)$ and the right-hand side of (16) has been averaged to be close to

$$(w_v(jh, (k + 1/2)\Delta t))^2 + w(jh, (k + 1/2)\Delta t)w_{vv}(jh, (k + 1/2)\Delta t).$$

The averaging has been done in such a way as to make w_{j+1}^{k+1}, w_{j-1}^{k+1} and w_j^{k+1} appear linearly. This averaging gives (16) two nice properties. First, if a solution of (14) is inserted in (16), and everything is expanded in a Taylor series about $(jh, (k + 1/2)\Delta t)$, then equality of the right- and left-hand sides follows up to terms of order $0(h^2)$ and $0(\Delta t^2)$. That is, the scheme is accurate to second-order in both time and space. In practice, this means that the difference between the computed w_j^k and $w(jh, k\Delta t)$, the true solution at the mesh points, will be $0(h^2) + 0(\Delta t^2)$. Second, (16) is a linear system of equations for the w_j^{k+1}. In fact, equation (16) is equivalent to

$$\begin{aligned} w_{j+1}^{k+1}\left(-\frac{\Delta\tau}{4h^2}(w_{j+1}^k - w_{j-1}^k) - \frac{\Delta\tau}{2h^2}w_j^k\right) \\ + w_j^{k+1}\left(1 - \frac{\Delta\tau}{2h^2}(w_{j+1}^k + w_{j-1}^k - 2w_j^k) + \frac{\Delta\tau}{h^2}w_j^k\right) \\ + w_{j-1}^{k+1}\left(\frac{\Delta\tau}{4h^2}(w_{j+1}^k - w_{j-1}^k) - \frac{\Delta\tau}{2h^2}w_j^k\right) = w_j^k . \end{aligned} \tag{17}$$

This has the form

$$A_j w_{j+1} + B_j w_j + C_j w_{j-1} = D_j \qquad j = 1, 2, \cdots, J - 1, \tag{18}$$

with $w_J = a$ and $w_0 = w_1$, reflecting the boundary conditions. This is a tridiagonal system of equations for the w_J and may be solved quite efficiently using Gaussian elimination (see Ref. 4, pp. 198–201). The method is easily described. Let

$$w_j = E_j w_{j+1} + F_j \tag{19}$$

for $j = 0, 1, \cdots, J - 1$. Replacing w_{j-1} by $E_{j-1}w_j + F_{j-1}$ in (18) gives w_{j+1} in terms of w_j. Comparing this relation with (19) gives

$$\begin{aligned} E_j &= \frac{-A_j}{B_j + C_j E_{j-1}} \\ F_j &= \frac{D_j - C_j F_{j-1}}{B_j + C_j E_{j-1}} \end{aligned} \tag{20}$$

for $j = 0, \cdots, J - 1$. Since $w_1 = w_0 = E_0 w_1 + F_0$ we see that $E_0 = 1$

and $F_0 = 0$. This completely determines $w_0, \cdots, w_J$ using (20) for $j = 1, \cdots, J-1$, and then (19) for $j = J-1, \cdots, 0$.

IV. RESULTS AND INTERPRETATION

In applying the results of this analysis to CCD operation, the most important operating characteristic is the amount of charge remaining behind after transfer from one plate to the next in a limited time. The remaining charge is plotted as a function of time in Fig. 6, using two different initial conditions, $Sq_0 = 10$ volts and $Sq_0 = 2$ volts. The nonlinear equation which has been solved reduces essentially to the diffusion equation after most of the initial q has been dissipated, and the solutions in this domain approach straight lines of log(charge) versus time when the average value of Sq is much less than $\kappa T/e$. However, at short time $\tau \lesssim 1$ the solution is effectively driven by the charge so the time rate of change for $Sq_0 = 10$ volts is roughly five times the time rate of change associated with $Sq_0 = 2$ volts. Between these two domains is a transition region where the average value of Sq lies between 0.2 $\kappa T/e$ and 5 $\kappa T/e$. Here the curves are very nearly

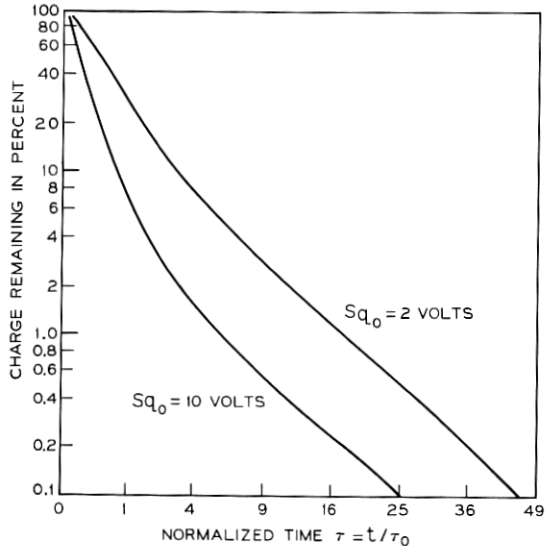

Fig. 6—The fraction of the charge remaining under the first plate as a function of the normalized time $\tau = t/\tau_0$. The abscissa is plotted as $\tau^{1/2}$, which spreads the region where $\tau < 1$, and leads to straight lines over the transition portion of the characteristic.

straight lines of log(charge) versus $\tau^{\frac{1}{2}}$. The different regimes reflect a feature mentioned when the equation was scaled; i.e., there is no single natural potential to use in forming the time scale. For very short times, the natural potential is the initial value of Sq. For times much greater than one, the natural potential is $\kappa T/e$. Figure 7 shows the transfer of charge with and without the aid of diffusion. It is clear that the last 0.1 volt of scaled charge receives a considerable boost from $\kappa T/e$.

In Fig. 6 it can be seen that in the vicinity of $\tau = 10$ the charge remaining diminishes to approximately 1 percent of its initial value, and in the vicinity of $\tau = 30$ the charge diminishes to 0.1 percent. These results are meaningless without some concept of the size of τ. Figure 8 helps to alleviate this shortcoming by showing τ_0 as a function of the plate width L for n-channel and p-channel devices. The n-channel mobility has been taken to be 750 and the p-channel mobility 150 cm²/volt-second.[5] From Fig. 8 it is possible to see that the values of τ_0 range from approximately 1 ns to 1 μs for plates ranging from 10 to 100 μm in width. To take a specific example, a 50-μm plate in a p-channel device would have a τ_0 of one-sixth of a microsecond. If operation were desired at a value of $\tau = 10$, aiming for a transfer

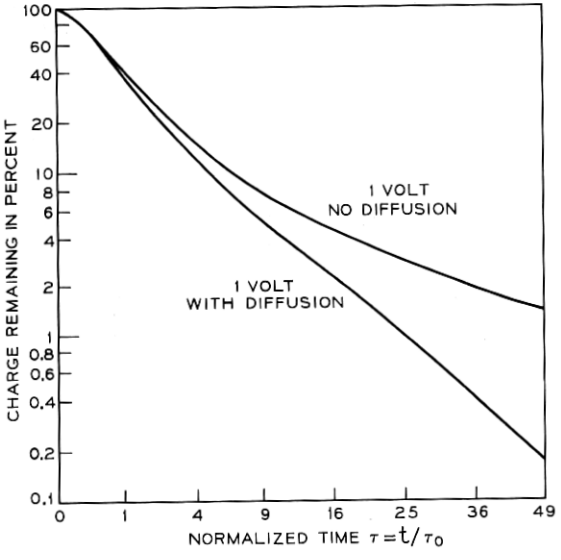

Fig. 7—The fraction of the charge remaining for initial values of $Sq_0 = 1$ volt with room temperature diffusion and no diffusion ($\kappa T/e = 0$).

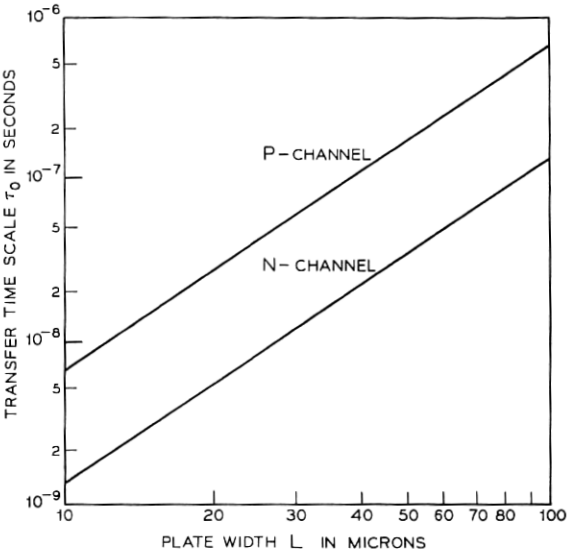

Fig. 8—A plot of the time scale factor τ_0 as a function of the CCD plate length L.

efficiency near 99 percent, then the operating frequency of a 2-phase CCD would be roughly 300 kHz, and the same loss per transfer would be achieved in a 3-phase CCD at 200 kHz. In an n-channel device with the same loss, those frequencies would increase to 1.5 and 1 MHz respectively.

In order to illustrate the effect of frequency, another example is shown in Fig. 9, where the loss per transfer is plotted as a function of clock frequency for a p-channel 2-phase CCD operating with square waves. In this type of operation, higher signal levels result in higher transfer efficiencies. The plate width in this case was chosen to be 25 μm, and at 1 MHz the loss per transfer ranges from about 0.3 percent for $Sq_0 = 10$ to 1.5 percent for $Sq_0 = 2$ volts.

The figures quoted so far must be regarded as worst-case loss figures. They apply to an isolated cluster of charge being propagated through a CCD. It will be possible to reduce this loss by approximately an order of magnitude by arranging the information propagated through the device in such a way that no information ever leads to a totally empty CCD cell. This will be effective, because for long times, i.e., $\tau > 10$, the charge remaining behind is substantially independent of the amount of charge initially put under a pad. This

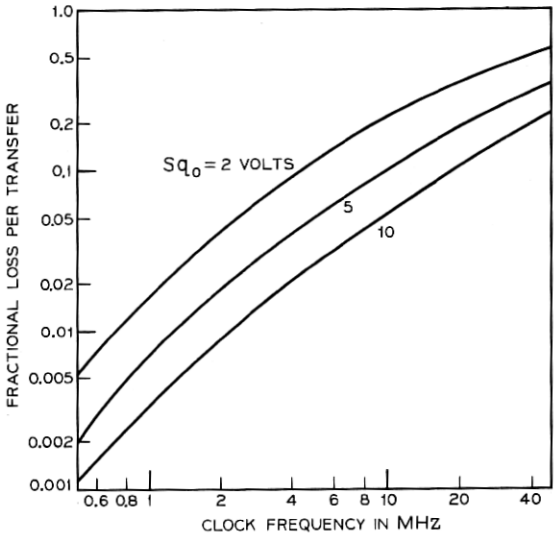

Fig. 9—The fractional loss per transfer of a P-channel 2-phase CCD, with a field-free length L of 25 μm, plotted against clock frequency with the initial ONE signal as a parameter. The ZERO's have no charge.

is illustrated by Fig. 10, which shows the absolute magnitude of remaining charge as a function of the charge which was initially placed in the device. In this figure, the amount of charge is described as its voltage equivalent *Sq*. The impact on device loss is illustrated in Fig. 11, where the loss per transfer for the same device shown in Fig. 8 is plotted as a function of the charge existing in a ZERO when a ONE contains 2 volts. It is presumed that the information carried is an alternating series of ONE's and ZERO's. This represents a worst-case condition when nonempty or "fat" ZERO's are used. From this figure, it is readily seen that a 2 to 1 ONE to ZERO ratio leads to practically an order of magnitude reduction in loss at a given frequency. Operation in this way requires the use of a threshold detector to ascertain whether a ONE or a ZERO was present; the success of such operation depends in large part upon the realization of a practical threshold detector.

The solution of the nonlinear diffusion equation also gives charge distributions in the CCD as a function of time. The charge distribution at selected times is shown in Fig. 12. Initially the left-hand end is almost totally undisturbed by the presence of an accepting well at the right-hand end of the CCD, but then as charge transfers out of

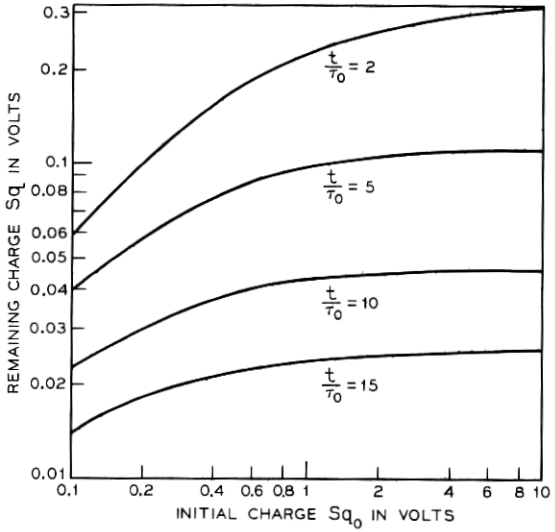

Fig. 10—The remaining charge at several times after the initiation of transfer presented as a function of the initial charge Sq_0.

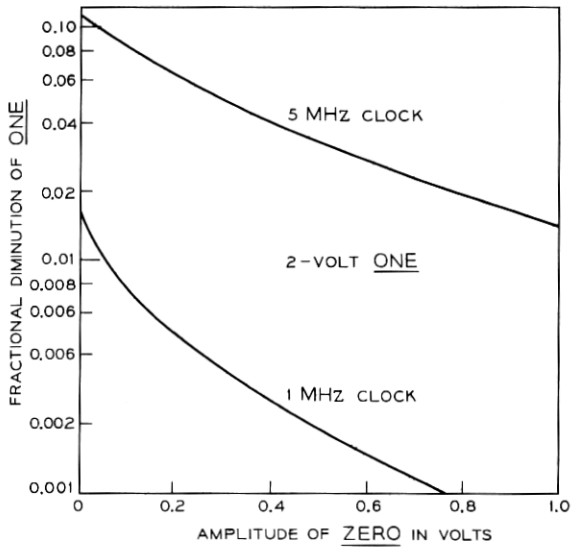

Fig. 11—The fractional diminution of a ONE as a function of the amplitude of a "fat" ZERO in an alternating series of ONE's and ZERO's. This example also refers to a 25-μm 2-phase p-channel CCD.

the device, the left end follows, but the profile which is established relatively early in the device cycle remains at least superficially unchanged through the course of the transfer.

If the potential of the source well is being changed at the same time the transfer is taking place, it is valuable to know the time development of the highest charge density in the source well, because it is necessary to prevent this point from ever reaching an injection condition. In this approximation injection occurs when $Sq \geq \gamma(V_A - V_{FB})$, and the well is no longer capable of holding the charge; the well and the substrate then form a forward biased p-n junction. For the example discussed before, the 25-μm p-channel CCD, the highest voltage in the well has been plotted as a function of time, assuming initial charges of 10 volts, 2 volts, and 1 volt; Fig. 13 shows the real time for the specified device and the general, normalized time. This figure shows that the potential on the plate must not drop to zero in a time less than 100 ns, if the injection of stored CCD charge into the bulk of the semiconductor is to be avoided.

It is unlikely that the initial charge configuration in a CCD will be perfectly square as assumed. To test the effect of this assumption

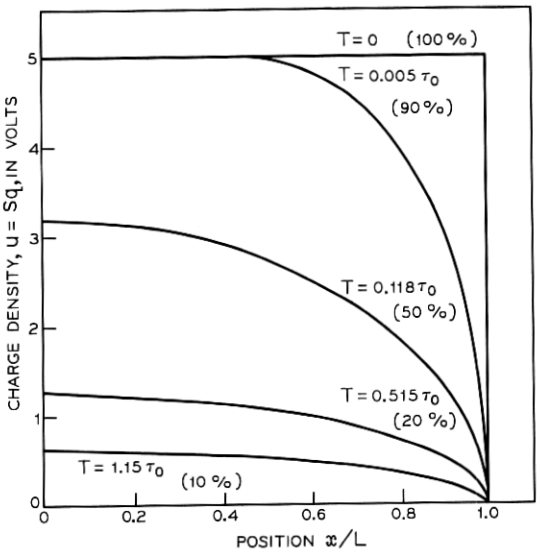

Fig. 12—The charge density as a function of position under the CCD plate, and the parameter is the time after initiation of transfer. The percentages refer to the total fraction of charge remaining under the plate.

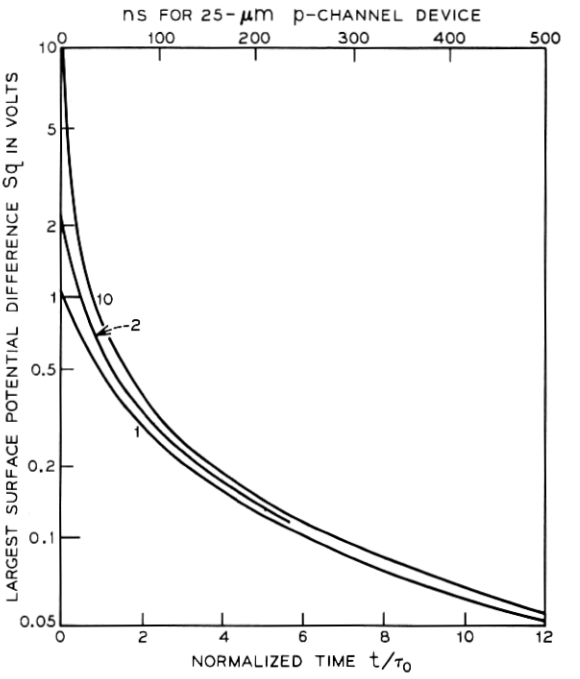

Fig. 13—The amplitude of the largest surface potential difference $Sq(0)$ as a function of time. Two time-axes have been provided, the generalized τ, and t for a 25-μm p-channel device.

on the results presented here, two initial conditions were used; one had charge distributed uniformly to an Sq value of 8 volts, and the other had charge distributed nonuniformly but having the same average charge density, that is $\overline{Sq} = 8$ volts. Figure 14 shows the difference in the charge remaining in the potential well as a function of time for these two distributions, and it is easily seen that beyond the time of $\tau = 0.25$ the two charge quantities are substantially identical.

The effect of finite carrier velocity at the transfer point was also tested. If infinite velocity cannot be achieved, the charge density at the point L cannot be 0, but it must be that finite value which will allow current to flow out of the potential well at the saturation velocity. Using this fact, it is possible to write the charge density at L as a function of the time rate of change of the total charge in the well dQ/dt.

$$u(L) = Sq(L) = \frac{1}{v_s}\frac{dQ}{dt} = \frac{L}{v_s}\frac{d\bar{u}}{dt}. \tag{21}$$

Here v_s is a saturation velocity and, assuming its value to be 10^7 centimeters per volt-second, the solution of equation (10) was reprogramed to reflect a value $u(L)$ in accordance with equation (21). The difference caused in the result was negligible, but because of the L^2/μ time scaling, it was more significant for very small plates than for the larger plates. The time error is shown in Fig. 15 as a function of charge remaining beneath the plate.

V. DISCUSSION

We have developed an equation governing charge transfer in flat-plate CCD's and shown how it can be solved numerically by an unconditionally stable finite difference routine. These solutions have been applied to the calculation of the properties of CCD's subject to certain constraints; the most serious of these limitations is the assumption of the instantaneous creation of the transferring condition. This assumption transforms into physical reality as the use of square-

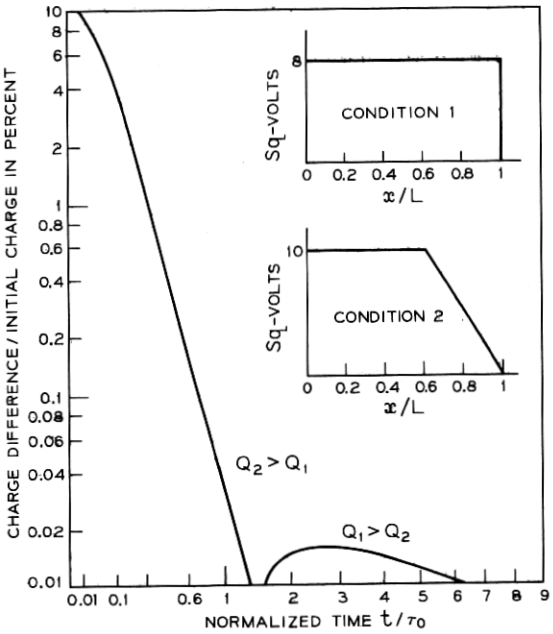

Fig. 14—Two initial conditions are compared to evaluate the impact of non-uniform distribution of a given total charge on the transfer predictions. The ordinate is the fractional difference in the total remaining charge and the abscissa is normalized time.

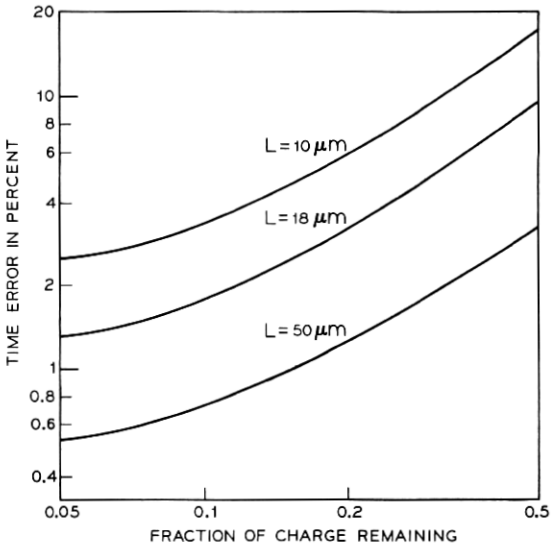

Fig. 15—An illustration of the effect of limiting the carrier velocity at $x = L$ to 10^7 cm/s, expressed as an error between the time predicted in the idealized case and the time in the velocity-limited case.

wave driving. Under these conditions, we have shown that with empty ZERO's losses of the order of 1 percent can be achieved in the vicinity of 1 MHz in p-channel CCD's, and the same order of loss at 5 MHz in n-channel CCD's. Further it has been shown that the use of "fat" ZERO's can effectively reduce this loss by as much as an order of magnitude. The problem which has not been solved here is that which arises when the accepting well is not created instantaneously but moves down with a finite time-rate of potential change. In this situation, a ONE will have a longer time in which to transfer than a ZERO will. This may tend to reduce the amount of charge left behind by the ONE as contrasted with that left behind by a ZERO. This would diminish the loss. At this stage, it is evident that losses of realizable CCD's, i.e., those with plates in the range of 15 to 25 μm, will be modest in the 5 to 10 MHz range, particularly if they are made using an n-channel technology. Using properly loaded ONE's and ZERO's, short shift registers should deliver useful signals, even clocked at 50 MHz.

This analysis has also shown that the existence of field-free regions in CCD's represents a considerable limitation on their performance. It will be possible to further lower losses by arranging substantial

penetration of transverse electric fields under the plates so that the charge transfer is limited by drift rather than diffusion. In this case, the scattering limited velocity assumes an important role.

CCD's on 10 Ω-cm substrates appear, on the basis of preliminary measurements,[3,6] to behave according to the predictions of the space charge assisted diffusion theory.

VI. ACKNOWLEDGMENT

The authors are indebted to G. E. Smith and J. McKenna for their stimulating suggestions, and to J. A. Morrison for his constructive comments.

REFERENCES

1. Boyle, W. S., and Smith, G. E., "Charge Coupled Semiconductor Devices," B.S.T.J., *49,* No. 4 (April 1970), pp. 587–593.
2. Amelio, G. F., Tompsett, M. F., and Smith, G. E., "Experimental Verification of the Charge Coupled Device Concept," B.S.T.J., *49,* No. 4 (April 1970), pp. 593–600.
3. Tompsett, M. F., Amelio, G. F., and Smith, G. E., Appl. Phys. Letters, *17,* 1970, p. 111.
4. Richtmeyer R. O., and Morton, K. W., *Difference Methods for Initial Value Problems,* 2nd Ed., New York: Interscience, 1970.
5. Murphy, N. St. J., Berg, F., and Flinn, I., Solid State Elect., *12,* 1969, p. 775.
6. Berglund, C. N., and Powell, R. J., private communication.

(*Added in proof.*) A related analysis with more limited scope than that above has been published by W. E. Engeler, J. J. Tiemann, and R. D. Baertsch in *Applied Physics Letters, 17,* 1970, p. 469.